

# Reservoir Rim Slope Stability Due To Rainfall And Operation Of Susu Dam

Jimjali Ahmed, Ahmad Fadli Mamat, Mohd Raihan Taha, Mohd Syazwan Md Rahim, Mohd Anuri Ghazali

**Abstract:** Susu Dam, in Cameron Highlands, is one of the dams in Malaysia with major fluctuation during operation. Leryar Village, which is a settlement of about 400 aborigines, is located on the bank and a rim slope failure could be catastrophic to the community. As such, this study investigates the landslide hazards due to the fluctuation of the reservoir and intense rainfall by conducting soil investigation, hazard mapping and advanced laboratory tests. Tests were conducted to obtain the hydraulic and mechanical properties of the soil, in the saturated and unsaturated states, which are necessary to simulate rapid drawdown and rainfall-induced shallow slides. Results of the slope stability analyses using this method differ greatly from the methods normally used by practitioners. Conventional methods would conclude that the slopes are sufficiently stable with Factor of Safety (FOS) values of at least 1.47, while this method, which involves rigorous testing and numerical modeling, resulted in an FOS of as low as 0.37. This implies the need to conduct extensive soil tests and apply the latest theories in soil mechanics to obtain reliable FOS for shallow failures involving transient flow conditions, such as rapid drawdown and rainfall infiltration. Aerial hazard map, using a qualitative approach, also agrees well with the FOS of the specific slopes. This suggests that a qualitative method of estimating landslide hazard could be used as a precursor to the advanced laboratory testing and slope stability analysis, which is costly and time consuming.

**Index Terms:** Landslide, Slope stability, Transient flow, Unsaturated soil, Rainfall-induced slides, Rapid drawdown, Hazard map.

## 1. INTRODUCTION

Dam failures due to rim slope instability could have extremely catastrophic consequences. An example is the Vajont Dam, Italy incident in 1963 where a massive landslide caused a mega-tsunami which claimed 1,910 lives [12]. Susu Dam, located in Cameron Highlands, Pahang, is one of the dams in Malaysia with major fluctuation during its operation. Having an operational fluctuation of 5m with a frequency of twice per day and an extreme drawdown of 24m, coupled with heavy rainfall, increases the probability of slope instability. The right bank of the slope (looking downstream) is currently inhabited with approximately 400 people and a rim slope failure could be catastrophic to the community especially during an extreme event. As such, this study investigates the probability of slope failure due to the fluctuation of the dam and intense rainfall by conducting hazard mapping and extensive soil investigation. Laboratory tests were conducted to determine the Soil Water Retention Curve (SWRC) and the failure envelope in the saturated and unsaturated states, which are required to conduct numerical simulation of rapid drawdown and rainfall-induced shallow slides. Cases such as the Three-Gorges Dam in China [4] and Punatsangchu-I Hydroelectric Project in Bhutan [13] are being taken into consideration in this study.

- Jimjali Ahmed, currently pursuing doctorate programme in civil engineering at Universiti Kebangsaan Malaysia, E-mail: jimjaliahmed@gmail.com
- Ahmad Fadli Mamat, Leader of this research project, Civil & GIS Unit, TNB Research Sdn Bhd, Malaysia
- Mohd Raihan Taha, Professor, Faculty of Engineering and Built Environment, Universiti Kebangsaan Malaysia
- Mohd Syazwan Md Rahim, Senior Geotechnical Engineer, Dr Nik and Associates Sdn Bhd, Malaysia
- Mohd Anuri Ghazali, Director, Geo Mag Engineering, Malaysia

## 2.1 Site Location

Susu Dam is part of the Ulu Jelai Hydroelectric Project undertaken by the national power company, Tenaga Nasional Berhad (TNB) which could generate 372MW. According to the United Nations, this project will be able to reduce carbon emission by 250,000tons per annum by replacing power plants that are using fossil fuel. The construction works commenced in 2011 and was completed in 2016. Its main dam (Fig. 1) with a height of 88m is located about 200km north of Kuala Lumpur, (coordinates 4°25'59.05"N, 101°32'27.79"E) and was built on the Bertam River using 750,000m<sup>3</sup> of Roller-Compacted Concrete (RCC). It is located within the Ulu Jelai and Bukit Jerut forest reserves, near Cameron Highlands-Lipis district border [14].



**Fig. 1.** Susu Dam which was constructed using roller-compacted concrete (Utusan Online).

The site is accessible via a federal road constructed by the Public Works Department of Malaysia (PWD). Slopes facing the dam, i.e. the right bank looking downstream, have been treated with rock revetment to improve stability. Leryar Village which is a settlement of about 400 aborigines is also located on the right bank (Fig. 2). There are concerns on the stability of the left bank, which has not been treated and could endanger the occupants of this village.



**Fig. 2.** Aerial view of Leryar Village and the road constructed by PWD, looking downstream, before the impoundment of the dam on 18<sup>th</sup> January 2016 (TNB Research Sdn Bhd).

## 2.2 Geology and Subsoil Profile

Cameron Highlands is located within the central part of the main range of Peninsular Malaysia that is underlain by granite. It consists, predominantly, of late Triassic intrusive biotite granite and roof pendants of lower Paleozoic sedimentary rocks intruded by minor quartz dykes. The main range granite crystallized in the late Triassic. Eight boreholes were carried out to determine the subsoil profile and obtain samples for classification tests. Standard Penetration Test (SPT) tests at every 1.5m depth were also conducted throughout the boreholes. Due to difficulties in obtaining undisturbed samples, which is crucial to determine hydraulic and mechanical properties, samples were obtained using large circular pipes next to the boreholes. The classification tests and SPT-N values from the BHs indicate that the site generally comprises of 1.5m to 6.0m, with an average thickness of 4.5m, very stiff sandy silt underlain by very hard (SPT-N Values > 50 Blows) silty sand with traces of gravel.

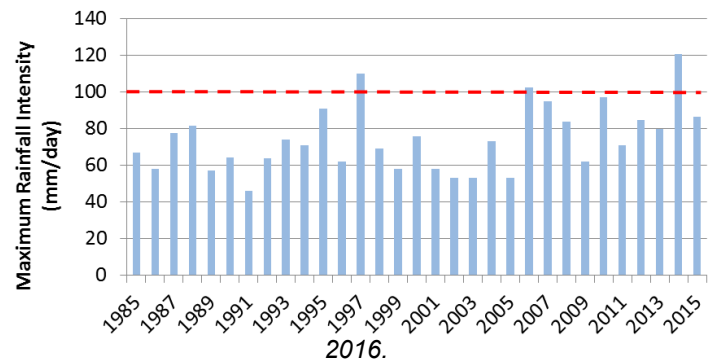
## 2.3 Groundwater Conditions and Rainfall Pattern

Groundwater depths measured from the top of boreholes initially range between 3.0m to 6.30m below the ground level. Standpipe piezometers, which provided monthly readings, show that the groundwater level could drop between 9m to 27m. The following water levels for the Susu Dam are established by TNB:

- Maximum Water Level (MWL), dam crest level = 548m
- Full Supply Level (FSL), spillway crest level = 540m
- Maximum Operating Level (MOL) = 530m
- Extreme Minimum Operating Level (EMOL) = 524m

Based on this information, it is possible to have a lowering of the water table of 6m during normal operations and 24m during an extreme event. The rate of drawdown greatly depends on the dam operations. As such, 2 drawdown rates are assumed in the analyses to cover for the possible ranges of drawdown during an extreme event. The nearest automated rain gauge is located about 16.7km northwest of the site, at Boh tea plantation (Station No 4414037). The 30-year pattern of the annual maximum rainfall intensity since 1985 is depicted in Fig. 3. It indicates that an intensity of more than 100mm/day is likely to occur once in every 10 years.

**Fig. 3.** Maximum daily rainfall intensity between 1985 till



## 2.4 Landslide Hazard Map

A landslide hazard map is produced for the left bank (looking downstream) of the Susu Dam using landslide hazard zonation method proposed by Anbalagan et al [1], [2], [3]. Slopes were first inventoried so that their boundaries and properties such as gradient and height could be determined. A total of 263 slopes were identified; 130 are natural terrains, 69 are cut slopes and 64 are embankments. Field assessments were then conducted and analyses on topography were carried out using ArcGIS. Hazard maps produced using this method are as shown in Fig. 4(a) and Fig. 4(b). A total of 115 slopes are categorized as very high to high hazard while the others are categorized as moderate to low hazard. Also shown, are the maximum and minimum water levels during operations and the cross sections selected for the slope stability analyses.

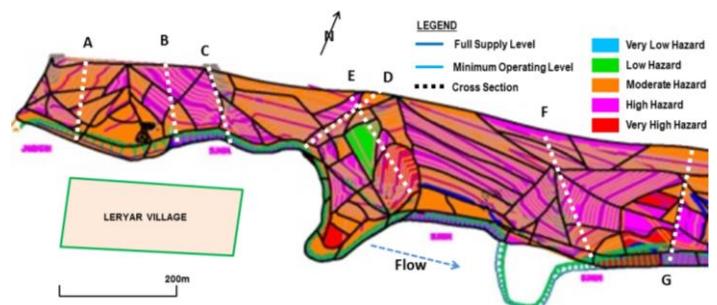


**Fig. 4(a).** Hazard map of left bank.

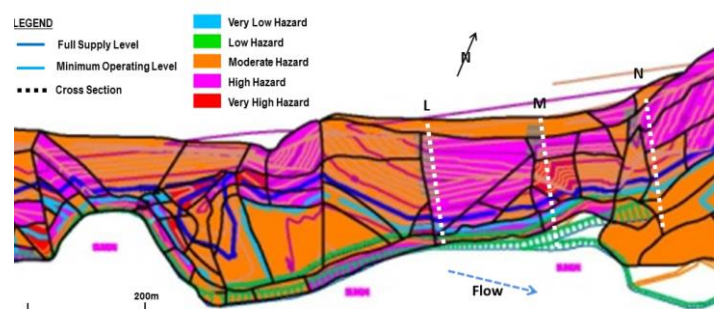


**Fig. 4(b).** Hazard map of left bank (cont'd).

## 3 HYDRAULIC AND MECHANICAL PROPERTIES

### 3.1 Hydraulic Properties

A coefficient of permeability of  $3.5 \times 10^{-5}$  cm/s, obtained from 8

falling head tests conducted on block samples, was used to represent the permeability value for the saturated state ( $k_{sat}$ ). In an unsaturated or partially saturated state, however, permeability will reduce with moisture content. In an unsaturated condition, soil comprises at least 3 phases; solid, water and air. Fredlund and Morgenstern [5] further introduced a fourth phase called the air-water interface. This air-water interface, also known as suction, is the natural ability of the water to exert a tensile pull, or surface tension. To explain the effect of suction in unsaturated soils, the determination of a soil property to describe its ability to attract and retain water is essential. This unique hydrological characteristic relationship is normally clarified based upon graphical approach, defined as the Soil Water Retention Curve (SWRC) or sometimes also known as the Soil Water Characteristic Curve (SWCC). The curve presents the relationships between water content and matric suction. The SWRC obtained using the pressure plate apparatus is shown in Fig. 5. It shows a saturated volumetric water content ( $\theta_{sat}$ ) of 0.43 which reduces to 0.28 after the imposition of 215kPa suction. The derivation of the predicted permeability function was then produced using SEEP/W based upon this SWRC, as shown in Fig. 6, which was derived using Van Genuchten's [15] equation.

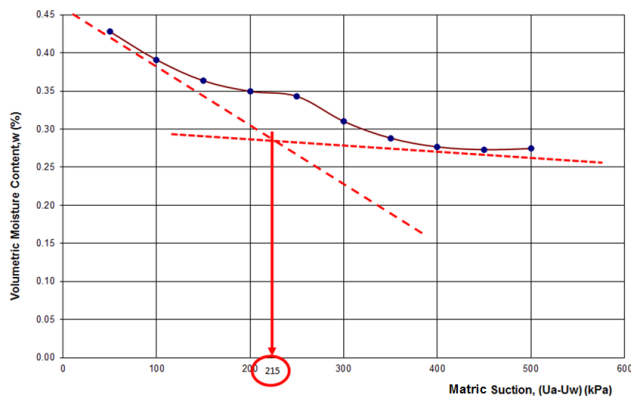


Fig. 5. Soil Water Retention Curve (SWRC).

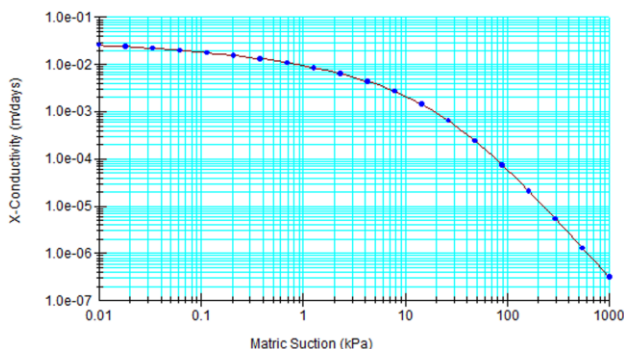


Fig. 6. Permeability function based on Van Genuchten's equation [15].

### 3.2 Mechanical Properties

A flat failure envelope, which could be represented with a constant cohesion and friction angle, is normally assumed in slope stability analyses. This should suffice for a deep-seated, but not for shallow failures. As such, researchers such as Md Noor et al [9], [10] and [11] proposed a curvilinear strength envelope instead. To properly define a bilinear failure envelope, 4 sets of triaxial Consolidated Drained (CD) test

were conducted. Four samples instead of the normal 3 samples for each set, were tested. The effects of long-term soaking due to the impoundment of the dam was also investigated by conducting another 4 sets of similar tests, but with the period of saturation much longer than usual. This was done by maintaining a back pressure slightly lower than the confining pressure for 2 weeks. Table 1 summarizes the mechanical properties from the extensive saturated CD tests assuming a bilinear failure envelope. Also shown in the table are the average strength parameters from 8 conventional triaxial Consolidated Undrained (CU) tests, which would normally be used by engineers in their analyses.

Table 1. Summary of conventional CU and extensive CD tests.

Type of Test	Average Strength Envelope Parameters			
	$c'$ (kPa)	$\phi'_{min}$ (degree)	$\phi'_{max}$ (degree)	$\phi'_t$ (kPa)
Conventional CU	4.5	32.6	-	-
Extensive CD	12.2	27.5	37.7	90.2
Extensive CD + Soaking	28.5	22.2	37.2	92.5

- $c'$  = conventional effective cohesion
- $\phi'_{min}$  = minimum / conventional effective friction angle with intercept  $c'$
- $\phi'_{max}$  = maximum friction angle with intercept equals 0
- $\phi'_t$  = transition effective normal stress from curvilinear to linear

The results suggest a much different strength parameters compared to the conventional CU tests. Soaked samples have a lower friction angle but a higher cohesion when normal stress exceeds about 90kPa based on the extensive CD tests. However, at lower normal stress, the friction angles for the normal and soaked samples are of about the same value. As the thickness of the topsoil layer, which could slide, is at most 6.5m thick, the effective overburden pressures would mostly be less than 90kPa. A friction angle,  $\phi'$  of  $37^\circ$  with a cohesion,  $c'$  equals zero would therefore be appropriate for slope stability

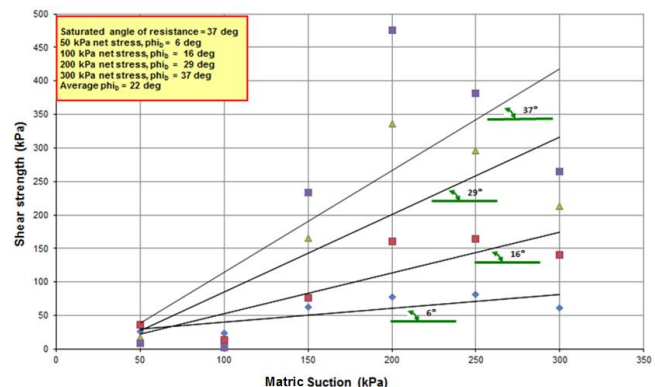


Fig. 7. Determination of the total value of C for 300kPa matric suction.

analyses.

With the presence of air components in the soil mass, the additional term of pore-air pressure,  $u_a$  must be included to describe the mechanical behavior of unsaturated soil. Fredlund and Morgenstern [6] proposed the concept of segregating these two stress states independently, known as the Extended Mohr-Coulomb failure surface. Equation 1 presents the constitutive equation, which is based on the independence of the stress state variables.

$$\tau = c' + (\sigma - u_a)\tan\alpha^a + (u_a - u_w)\tan\alpha^b \tag{1}$$

where,

- $\tau$  = shear strength
- $c'$  = effective cohesion of the soil
- $\alpha^a$  = friction angle with respect to changes of net stress
- $\alpha^b$  = friction angle with respect to changes of suction

Fredlund et al [7] further suggested that  $\alpha^a$  could be assumed to be equal to  $\alpha'$ . The interpretations of the results, by fixing  $\alpha^a$  equals  $\alpha'$ , were based upon the graphical method reported by [8]. They suggested that the suction term in the above shear strength equation,  $((u_a - u_w)\tan\alpha^b)$  for an unsaturated soil could be considered as contributing to the total cohesion (denoted as C). This total cohesion of each sample is then plotted against matric suction to obtain the gradient of the plots that represents  $\alpha^b$ . The expression for C shall be presented as follows:

$$C = c' + (u_a - u_w)\tan\alpha^b \tag{2}$$

And substituting Equation 2 into Equation 1,

$$\tau = C + (\sigma - u_a)\tan\alpha' \tag{3}$$

By using Equation 3, the calculation to derive both stress ratios can be implemented separately. Fig. 7 provides an example of obtaining the total value of C for each sample based on  $\tau$  against net stress ( $\sigma - u_a$ ) for a matric suction of 300kPa. These graphs show that each line is parallel, reflecting a gradient equals to  $\alpha'$ , i.e.  $37^\circ$ . Six tests with suctions ranging from 50kPa to 300kPa (4 shearing stages each) were conducted for this purpose. The total cohesions were then plotted against suction to obtain the best fit gradient of the plots that represents  $\alpha^b$ , which indicates an average value of  $22^\circ$  (refer to Fig. 8).

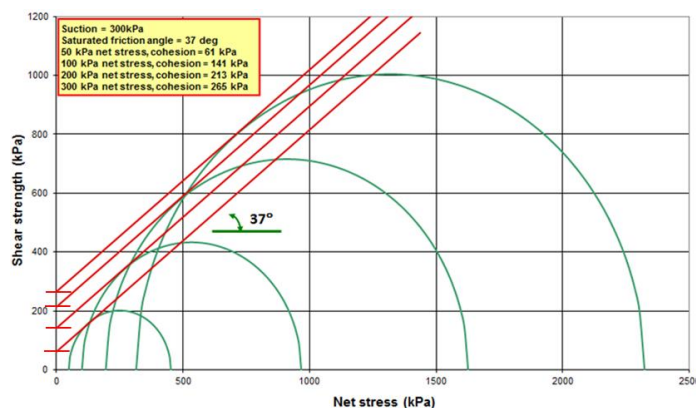


Fig. 8. Total cohesion with matric suction (determination of average  $\alpha^b$ )

## 4 SLOPE STABILITY ANALYSIS

### 4.1 Methodology

A total number of 10 cross sections, as indicated in Fig. 4(a) and Fig. 4(b), were selected for analyses. Each section is different in geometry as well as stratigraphy, which were

defined based on the nearest boreholes location and survey profile. Also, several series of mesh refinement procedures were carried out in order to capture the region with the largest displacement on the slope. This procedure was targeted to prevent possible numerical instabilities during iteration. The size of the mesh was set to be 2-meter length for each section. There are 3 numerical case studies that have been carried out for each cross section. In each case, the finite elements software, SEEP/W was initially used to obtain a steady state condition of the groundwater table. Then, a total number of 10 days was set for transient analysis to simulate the rapid drawdown and rainfall with time. Ultimately, SLOPE/W (limit equilibrium method) was used for each pre-defined time stepping in order to investigate the variation of Factor of Safety (FOS) against time. The details of each case are as follows:

- Case 1: fast drawdown (MWL to EMOL in 6.6 days) without rain
- Case 2: fast drawdown (MWL to EMOL in 6.6 days) with intense rain
- Case 3: slow drawdown (MWL to EMOL in 40 days) with intense rain

For cases 2 and 3, the surface boundary condition with rainfall was included in the analyses to investigate the cumulative effects of infiltration and drawdown process. A rainfall intensity of 100mm/day and duration of 1.5days was assumed for these cases. Table 2 presents the summary of the hydrological and mechanical properties used in the analyses. It should be noted that the value for  $\alpha'$  has been reduced from  $37^\circ$  to  $35^\circ$  for conservative measures.

Table 2. Summary of hydraulic and mechanical properties.

Soil Layer	Consistency	Density (kN/m <sup>3</sup> )	k <sub>sat</sub> (cm/s)	c' (kPa)	$\alpha'$ (°)	$\alpha^b$ (°)
Sandy Silt	Very Stiff	19	3.5x10 <sup>-5</sup>	0	35	22
Silty Sand	Hard	20	3.5x10 <sup>-6</sup>	150	42	22

### 4.2 Slope Stability Results

Table 3 presents the summary of the minimum factor of safety (FOS<sub>min</sub>) for each case. Also included are FOS<sub>min</sub> using conventional method for comparison. From the table, it can be seen that section C and section L exhibit low FOS values of 0.37 and 1.17, respectively; the rest are more than 1.82. Fig. 9 shows the variation of slope stability (FOS) against time or Section C.

Table 3. Summary of minimum FOS for each case and cross section.

Section	Conventional Method	Steady State Condition	Case 1	Case 2	Case 3
			Fast Drawdown	Fast Drawdown & Rain	Slow Drawdown & Rain
A	3.96	3.51	3.45	3.38	3.48
B	4.53	3.28	3.22	3.11	3.17
C	1.47	2.10	2.08	0.38	0.37
D	4.38	1.99	1.98	1.96	1.98
E	3.41	2.44	2.39	2.36	2.41
F	2.86	1.86	1.83	1.82	1.85
G	3.41	5.55	3.50	3.51	5.35
L	1.55	1.54	1.38	1.17	1.28
M	1.66	2.10	1.93	1.93	2.09
N	1.57	1.93	1.82	1.82	1.91

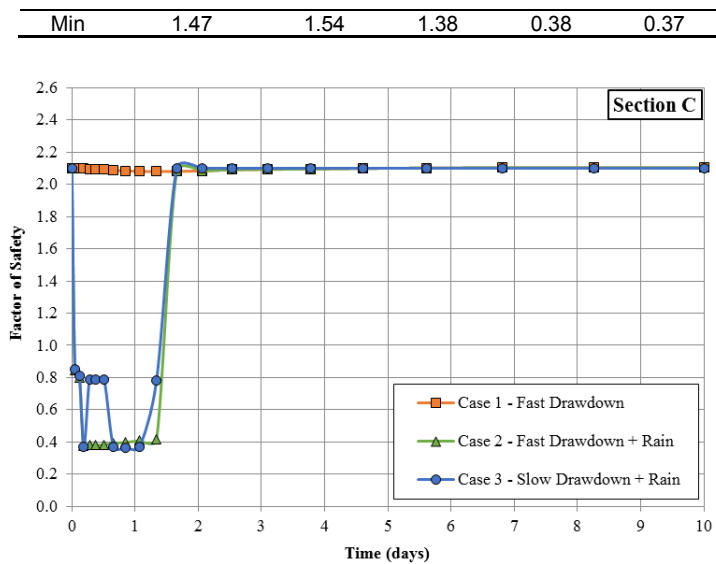


Fig. 9. Factor of safety variation with time for Section C.

## 5 CONCLUSIONS AND DISCUSSIONS

Extensive Triaxial Consolidated Drained (CD) tests yield different strength parameters from the conventional Consolidated Undrained (CU) tests, while CD tests on samples soaked or saturated for 2 weeks show lower friction angle at high confining pressures. Assuming a bi-linear strength envelope, The CD tests suggest a consistent friction angle ( $\phi'$ ) of  $37^\circ$  for effective confining pressures lower than 90kPa, regardless of soaking period. As the site comprised of 1.5m to 6.5m of completely weathered granite, shallow failures, instead of deep-seated failures are most likely to occur. Using this value as the friction angle is, therefore, more appropriate. Conventional slope stability method seldom considers rapid drawdown and rainfall infiltration due to the unavailability of the hydraulic and strength properties of the soil in the unsaturated state. Based on advanced unsaturated triaxial tests and the latest theories in unsaturated soil mechanics, the average friction angle for matric suction ( $\phi^b$ ) was estimated to be  $22^\circ$ . The relationship of permeability vs matric suction was also deduced based on saturated permeability ( $k_{sat}$ ) value of  $3.5 \times 10^{-5}$  m/s and the Soil Water Retention Curve. Slope stability analyses on 10 selected cross sections of the left bank, assuming 2 rates of drawdown and a rainfall intensity with a return period of about 1 in 10 years, resulted in a minimum Factor of Safety (FOS) which is much lower than the FOS derived from conventional method with 2 sections having FOS lower than 1.5, i.e. the minimum value normally required for dams. The results also suggest that intense rain, instead of rapid drawdown, is the main triggering factor of slope instability for Susu Dam. Further assessments were carried out to understand the mechanism that could lead to this failure state. The detail analyses show that section C could possibly fail even without impoundment and there is only slight decrease in FOS with a much lower permeability value for section L. This exhibit the potential hazard exposed for both sections. Although the assumption of having both drawdown and rainfall infiltration processes to happen simultaneously may be conservative, it would be prudent to provide precautionary measures for both sections, so as to prevent any catastrophic incident to happen due to extreme

climate changes. The treatment used by the Public Works Department (PWD) for the right bank, i.e. using rock revetment, may be considered for these 2 sections. It is also interesting to note that the aerial hazard map produced in this study agrees well with the slope specific stability analyses. Sections C and L are indicated as high hazard while sections A and G, with high FOS, are indicated as moderate hazard. Section F, however, has reasonable FOS but is indicated as high hazard in the map. This finding, nevertheless, suggests that a qualitative method of estimating landslide hazard could be used as a precursor to a detailed slope stability analysis, which may not only be costly but also time consuming.

## ACKNOWLEDGMENT

The authors wish to gratefully acknowledged TNB Research Sdn Bhd, Kumpulan Ikram Sdn Bhd, Ministry of Education Malaysia (via Universiti Kebangsaan Malaysia) for their financial and in-kind supports in completing the research study presented in this paper.

## REFERENCES

- [1] Anbalagan, R.: Landslide hazard valuation and zonation mapping in mountainous terrain. *Engineering Geology*, 32, 269-277 (1992).
- [2] Anbalagan, R., Chakraborty, D., Kohli A.: Landslide hazard zonation (LHZ) mapping on meso-scale for systematic town planning in mountainous terrain. *Journal of Scientific & Industrial Research*, 67, 486-497 (2008).
- [3] Anbalagan, R. Kumar, R.: Reservoir Induced Landslides – A case study of reservoir rim region of Tehri Dam. TIFAC-IDRiM Conference, New Delhi, India (2015).
- [4] Cojean, R., Cai, Y. J.: Analysis and modeling of slope stability in the Three-Gorges Dam reservoir (China) - The case of Huangtupo landslide. *Journal of Mountain Science*, 8(2), pp. 166–175 (2011).
- [5] Fredlund, D. G., Morgenstern, N. R.: Stress state variables for unsaturated soils. *Journal of Geotechnical Engineering Division, ASCE*, 103, pp. 447-466 (1977).
- [6] Fredlund, D. G., Morgenstern, N. R.: Stress State Variables for Unsaturated Soils. *Journal of the Geotechnical Engineering Division, ASCE* 104, pp. 415-1416 (1978).
- [7] Fredlund, D. G., Morgenstern, N. R., Widger, R. A.: Shear-Strength of Unsaturated Soils. *Canadian Geotechnical Journal*, 15, pp. 313-321 (1978).
- [8] Ho, D. Y. F., Fredlund, D. G.: Increase in strength due to suction for two Hong Kong soils. *Proceeding ASCE Specialty Conference Engineering and Construction in Tropical and Residual Soils*, pp. 263-295 (1982).
- [9] Md. Noor, M. J., Anderson, W. F.: A comprehensive shear strength model for saturated and unsaturated soils. *Proceeding 4th International Conference on Unsaturated Soils, ASCE Geotechnical Special Publication No. 147, Carefree, Arizona, Vol. 2, pp. 1992–2003 ISBN 0-7844-0802-5 (2006).*
- [10] Md. Noor, M. J., Hadi, B. A.: The role of curved-surface envelope Mohr-Coulomb model in governing shallow infiltration induced slope failure. *The Electric Journal of Geotechnical Engineering* (2010).
- [11] Md. Noor, M. J., Derahman, A.: Curvi-linear shear strength envelope for granitic soil grade VI, *Unsaturated Soils: Theory and Practice*, pp. 1–6 (2011).
- [12] Paronuzzi, P., Rigo, E., Bolla, A.: Influence of filling-drawdown cycles of the Vajont reservoir on Mt. Toc slope stability. *Geomorphology*, 191, pp. 75–93 (2013).

- [13] Sati, S. K., Khazanchi, R. N., Mishra, A., Gautam, A. K.: Reservoir rim stability: A case study of Punatsangchu- I H.E. Project, Bhutan. 7th Indian Rock Conference, pp. 300-309 (2017).
- [14] The Star Online, <https://www.thestar.com.my/business/business-news/2016/08/09>.
- [15] Van Genuchten, M. T.: A closed-form equation for predicting the hydraulic conductivity of unsaturated soil. Soil Science Society of America, 44, pp. 892-898 (1980).